Numerical analyses on the wall deflections of The Bow excavation

Greg Guangfeng Qu[1], KwanYee Lo[2], Matthew Janes[3], Silvana Micic[1] & Thomas Lardner[3]
1 TROW International Ltd., Brampton, Ontario, Canada
2 Geotechnical Research Centre, - The University of Western Ontario, London, Ontario, Canada
3 Isherwood Associates, Mississauga, Ontario, Canada

ABSTRACT
The construction of the Bow office tower involved an excavation approximately 100 m wide, 190 m long, and about 21 m below ground surface. This paper presents a finite element analysis of stress and displacement caused by the excavation, and then evaluates the influence of the shear band and the weak zone in rock by comparing the measured performance of the shoring system with the calculated.

RÉSUMÉ
La construction de la tour à bureaux Bow a nécessité une excavation d'environ 100 m de large, 190 m de long, et d'environ 21 m de profondeur. Cet article présente les résultats d'une modélisation numérique par la méthode des éléments finis du champ de contraintes et de la quantité de déplacement induits par l'excavation. Par la suite, l'influence des différentes valeurs de cisaillement et la zone de faiblesse dans le roc ont été évaluées en comparant les performances mesurées du coffrage avec les valeurs calculées.

1 INTRODUCTION

The proposed construction of The Bow office tower involved an excavation approximately 100 m wide and 190 m long, and about 21 m below ground surface. As shown in Figure 1, the excavation is adjacent to the Petro-Canada Centre, Calgary's Light Rail Transit, and The Royal Canadian Legion No.1. To permit The Bow excavation, a comprehensive shoring system was designed and constructed, together with an extensive monitoring program, which consisted of 12 inclinometers, 8 extensometers and precision target monitoring of the shoring wall and surrounding buildings. This paper presents a finite element analysis of stress and displacement caused by the excavation, and then compares the measured performance of the shoring system with the calculated.

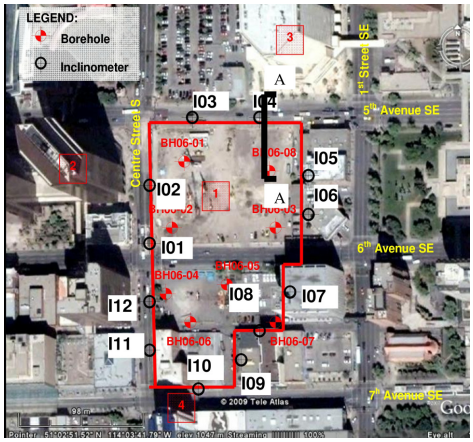

Figure 1. The Bow site: (1) The Bow; (2) Petro-Canada Centre; (3) Telus and (4) Calgary's Light Rail Transit (modified from Lo et al. 2009)

2 FINITE ELEMENT MODELLING

Initially, several softwares, including ABAQUS, AFENA, and PHASE2, were used to perform trial analysis, and it was found that results closely matched with each other and the PHASE 2 appeared to be the most convenient. A plane strain finite element model was developed using the finite element software, PHASE 2, to simulate the response of shoring system to The Bow excavation. As shown in Figure 2a, the finite element (FEM) model is 190 m wide and extends to a depth of 80 m. The base was modelled as a rough and rigid boundary, while the lateral boundaries were modelled as smooth and rigid. Figure 2b shows the finite element mesh, where 6271 three-noded elements were used to model the soil and rock materials. The caisson wall and tie-back anchors were modelled using beam elements and bolt elements, respectively.

2.1 Shoring System: Anchor and Caisson Wall

The shoring system of The Bow excavation mainly consists of seven layers of anchors, and a continuous caisson wall installed 2 m into the rock with a shotcrete wall beneath. Figure 3 shows the locations of the seven layers of anchors. The top two layers of anchors have a pre-tension force of 630 kN, and the rest are 360 kN. Table 1 presents the detailed anchor properties.

The caisson wall is modeled using a 0.8 m thick beam, which retains the 7m-thick soil layer and extends 2 m into the rock layer. The corresponding Young's modulus and Poisson's ratio are 10 GPa and 0.2, respectively. This numerical model doesn't take account of the effect of the shotcrete wall.

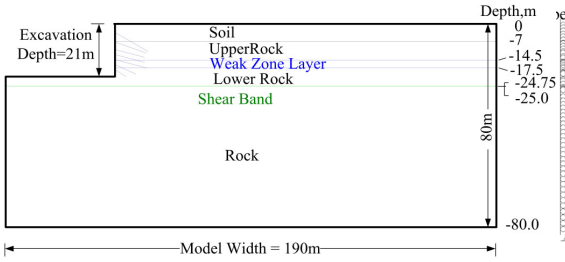

Figure 2a. Geometry of the 2D finite element model for the Bow excavation

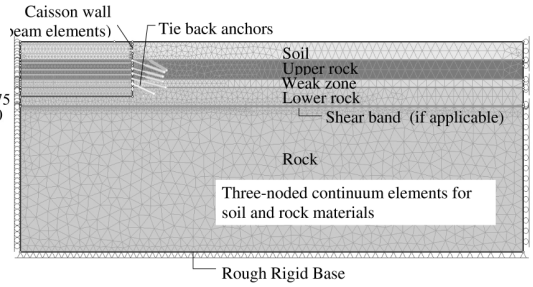

Figure 2b. Finite element mesh (see A-A cross section in Figure 1)

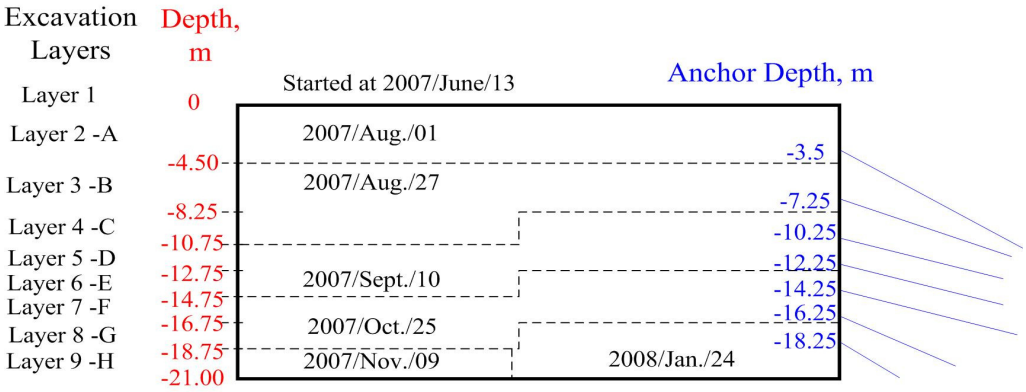

Figure 3. Location of anchors and excavation simulation (see A-A cross section in Figure 1)

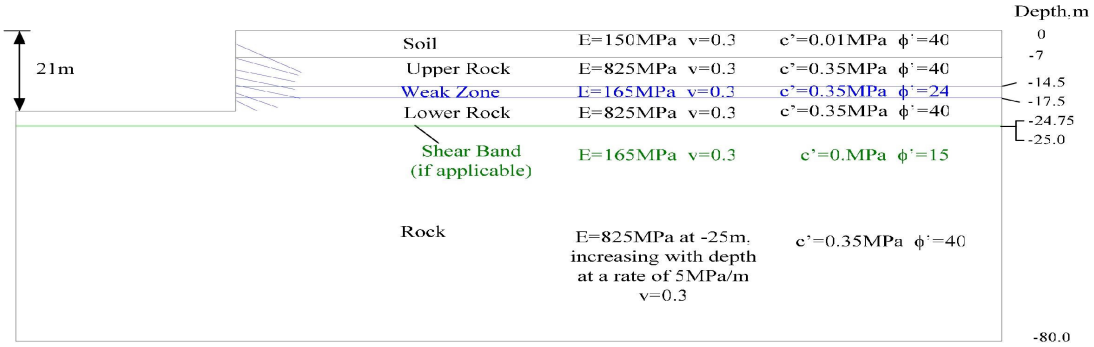

Figure 4a. Soil and rock layers and their engineering parameters

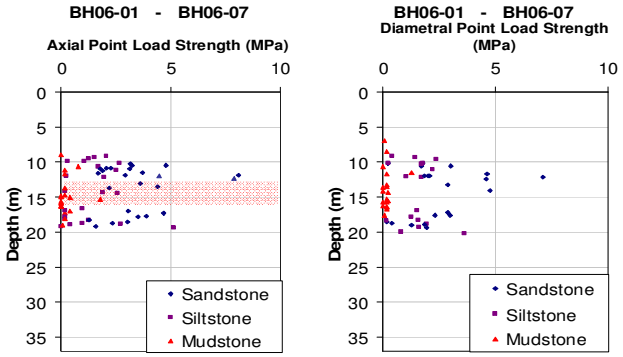

Figure 4b. Point load strength profile

Table 1. Anchor properties in analyses

Anchor No.	1[1]	2[1]	3[2]	4[2]	5[2]	6[2]
Pretension force (MN)	0.63	0.63	0.36	0.36	0.36	0.36
Tensile capacity (MN)	1.05	1.05	0.69	0.69	0.69	0.69
Total length (m)	15	13	12	12	13	9
Bonded ratio (%)	46	54	50	50	60	67
Depth (m)	3.50	7.25	10.25	12.25	14.25	16.25

[1]Lateral spacing is 2.1 m
[2]Lateral spacing is 3.0 m

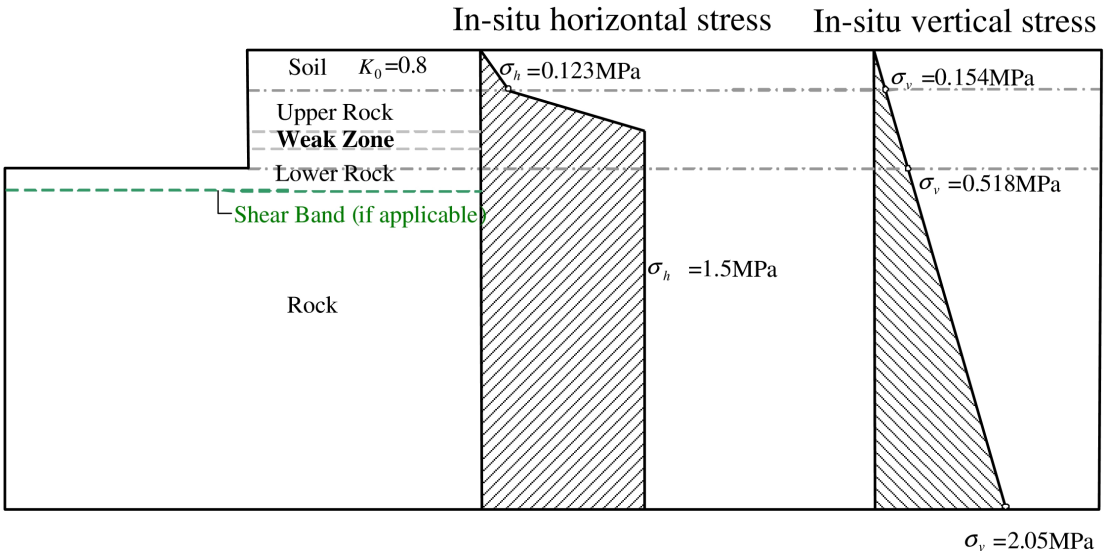

Figure 5. Distribution of the assumed vertical and lateral *in-situ* stresses

2.2 Soil and Rock Properties

Ground conditions were simplified for modelling by considering a 7 m thick soil layer (mainly well graded dense gravel and cobble) over the Porcupine Hill rock formation (mainly layered weak mudstones, siltstones, and sandstones). The rock formation has a 3 m thick weak zone between -14.5 m and -17.5 m, and a thin (0.25 m) shear band at a depth of -25 m (i.e., 4 m below the excavation bottom). Figure 4a shows the soil and rock layers and their corresponding properties.

It is noted that both the limited number of samples and the fractured and highly fissile nature of mudstone renders sampling and laboratory tests very difficult. The strength and deformation parameters for rock layers were estimated from the available laboratory tests, which were performed on the highly fissured mudstone specimens recovered within the excavation at a depth of 17.25 to 18.15 m (see Lo et al., 2009).

For rock material in the weak zone, the engineering parameters of c'=0.35 MPa, ϕ'=24°, and E=165 MPa were estimated from a series of direct shear and triaxial shear tests. The shear band was modeled using the measured residual strength parameters of c'=0 MPa and ϕ'=15° (see Lo et al., 2009).

Figure 4b shows the point load strength profile derived from AMEC report (2006). It can be seen that the upper rock, and lower rock layers appears much harder than the weak zone from 14.5 m to 17.5 m depth. Thus, a higher friction angle of ϕ'=40°, and Young's elastic modulus of E=825 MPa were assigned to the upper and lower rock layers. The underlying rock layer was assumed to have a friction angle of 40° and Young's elastic modulus increasing with depth at a rate of 5 MPa/m (see Figure 4a).

2.3 *In-situ* Stress

It appears that no stress measurement in the near surface rock formations in the Calgary area has been carried out. The state of stresses in the rock therefore has to be assumed based on experience elsewhere. This 2D plane strain numerical analysis assumes that the lateral *in-situ* stress is orientation-independent. Figure 5 shows the distribution of both vertical and lateral *in-situ* stresses. As shown in Figure 5, the vertical stress is calculated according to a unit weight of 0.022 MN/m^3 for the soil layer and 0.026 MN/m^3 for the rock layers. The lateral stress (σ_h) increases linearly with depth assuming K_o=0.8 in the soil layer. For the underlying layer, the lateral stress has a transition zone with σ_h increasing from 0.145 MPa to 1.5 MPa. Below this, a uniform lateral stress distribution is assumed (σ_h=1.5 MPa).

Further analysis will be carried out to analyze the orientation of major lateral principal stress.

3 RESULTS AND DISCUSSION

A parametric study on the 2D numerical model has been performed to investigate the influence of mesh density, boundary condition, *in-situ* stress, and the engineering parameters of soil and rock. With the results of this parametric study, a 2D plane strain model was constructed with appropriate finite element mesh and boundary conditions. The results of these numerical analyses are compared with the field monitoring results.

3.1 Numerical Model Accounting For Both Weak Zone and Shear Band

3.1.1 Deflection

Figure 6 presents the measured and calculated deflections at the inclinometers of #3 and #4 on the north side of The Bow excavation. The measured deflections indicate that 1) the influence of deep-seated shear band is significant, leading to an about 30 mm lateral movement within the thin shear band layer at the inclinometers #3 and #4; and 2) the weak zone from 14.5 m to 17.5 m depth introduced a bulging effect at its corresponding elevation. The calculated deflection, as shown in Figure 6, satisfactorily simulates the effects of shear band and weak zone (i.e., large lateral movement within the shear band and bulging effect at the weak zone elevation). In addition, the calculated and measured maximum lateral displacements were consistent in term of magnitude and corresponding elevation. Specifically, the maximum lateral displacements are 60 mm at a depth of 14.6 m at the #3 inclinometer, 51 mm at 16.4 m at the #4 inclinometer, and 60 mm at 15.0 m for the calculated, respectively.

For the soil layer, the measured deflections at different inclinometers exhibit two different trends. The measured deflections at #3 and #4 (see Figure 6) indicate a significant top-retaining effect; whereas the deflections at other inclinometers (#8, #9, #11, and #12) are approximately uniform or even show a cantilever-type of shape, as shown in Figure 7. The reason for this disagreement remains unknown. The numerically calculated lateral movement in the soil layer (see Figure 6) are generally uniform, agrees better with those observed at the inclinometers of #8, #9, #11, and #12.

Figure 6 also indicates one difference between the calculated and measured deflections: the measured lateral movement at a depth of 30 m at inclinometer anchorage is assumed to be zero, while the calculated is about 6 mm due to contribution from the rock below 30 m.

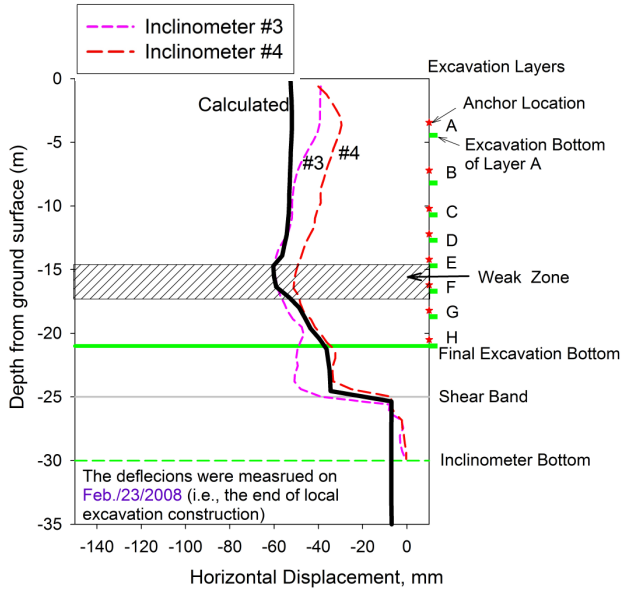

Figure 6. Calculated and measured resultant deflections at #3 and #4 on the north side

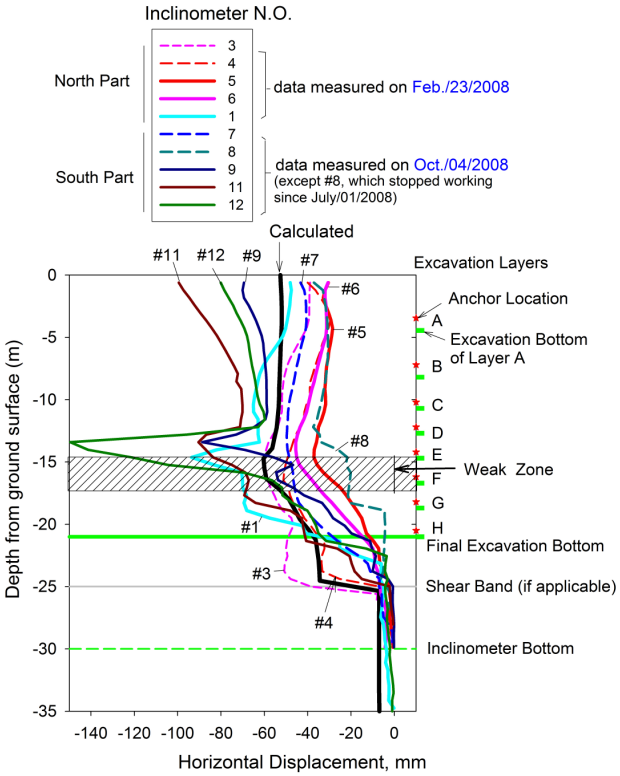

Figure 7. Calculated and measured resultant deflections at inclinometers including #3, #4, #8, #9, #11, and #12

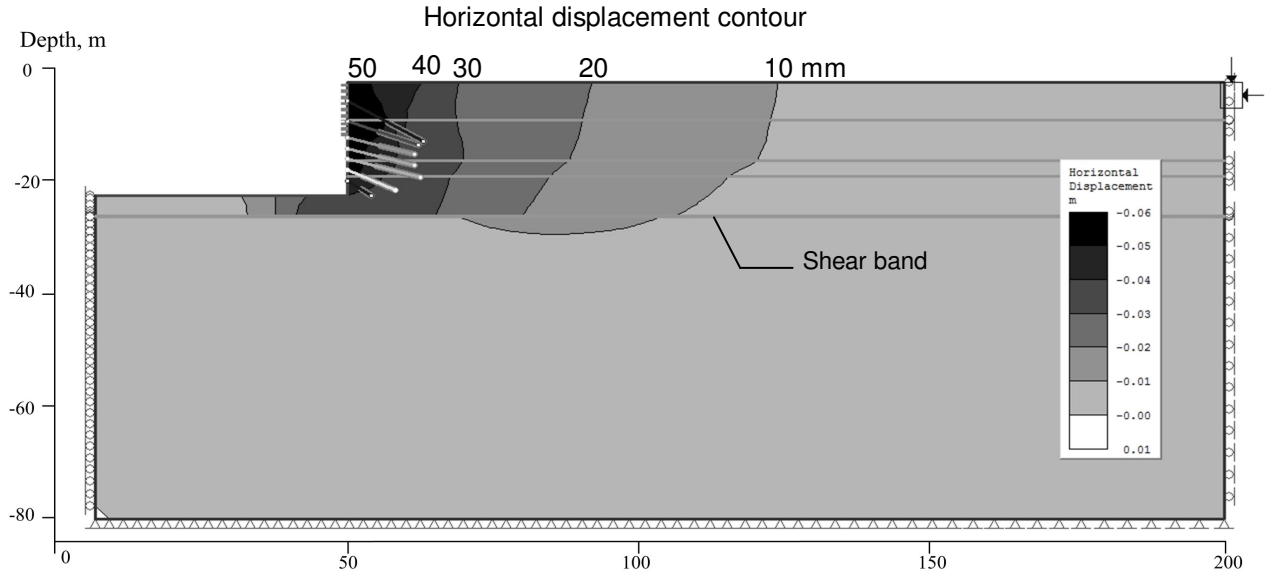

Figure 8. Horizontal displacement contour (calculated)

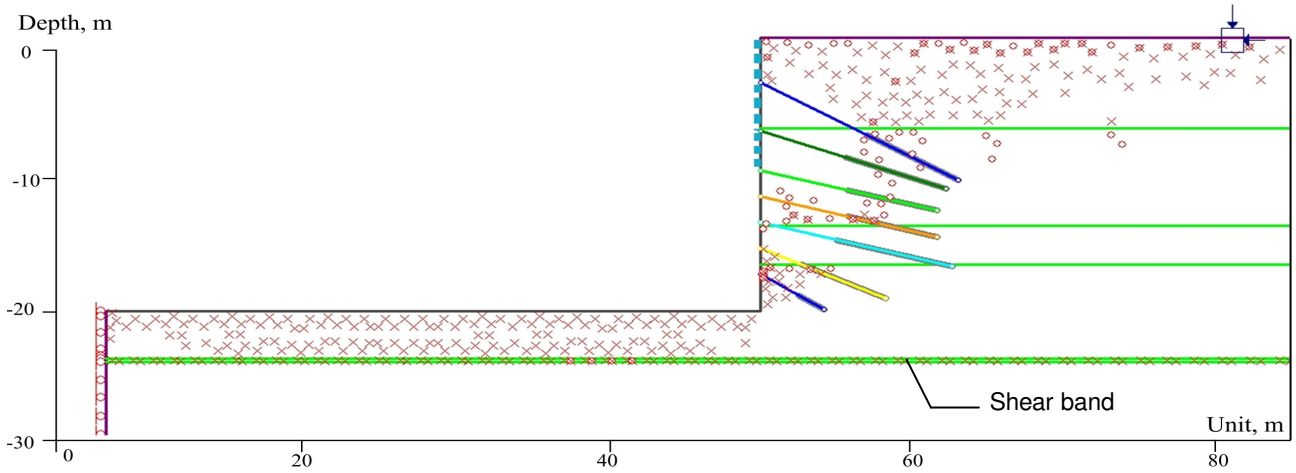

Figure 9. Plastic zone distribution from numerical analysis

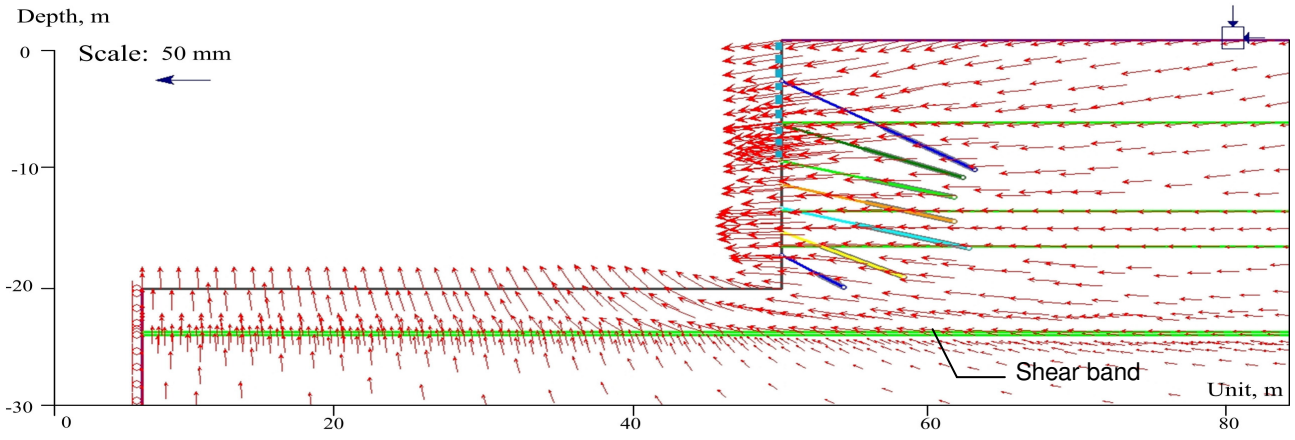

Figure 10. Total displacement vectors (calculated)

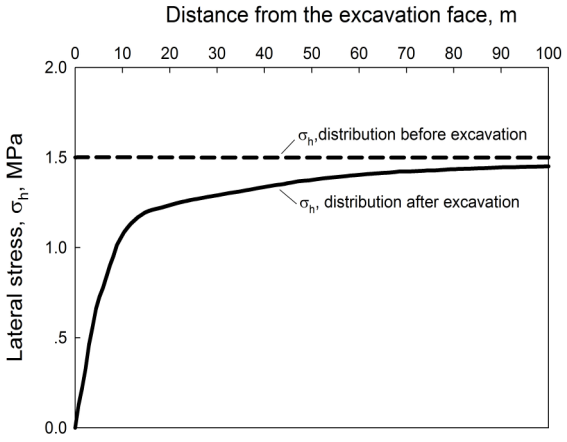

Figure 11. Redistribution of the lateral stress at the weak zone after excavation

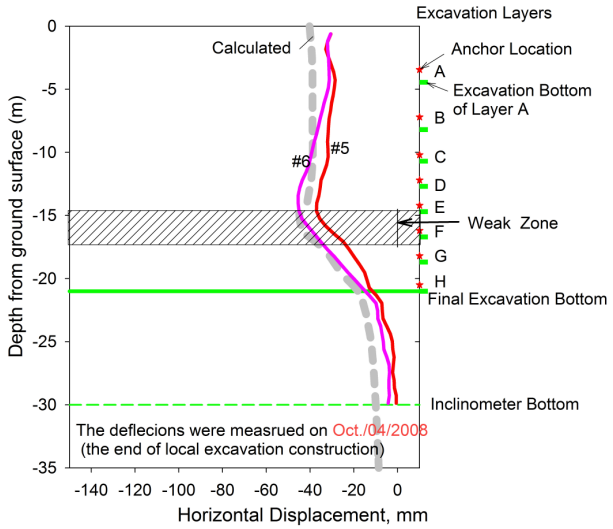

Figure 12a. Calculated and measured resultant deflections at #5 and #6 on the east side of the Bow excavation

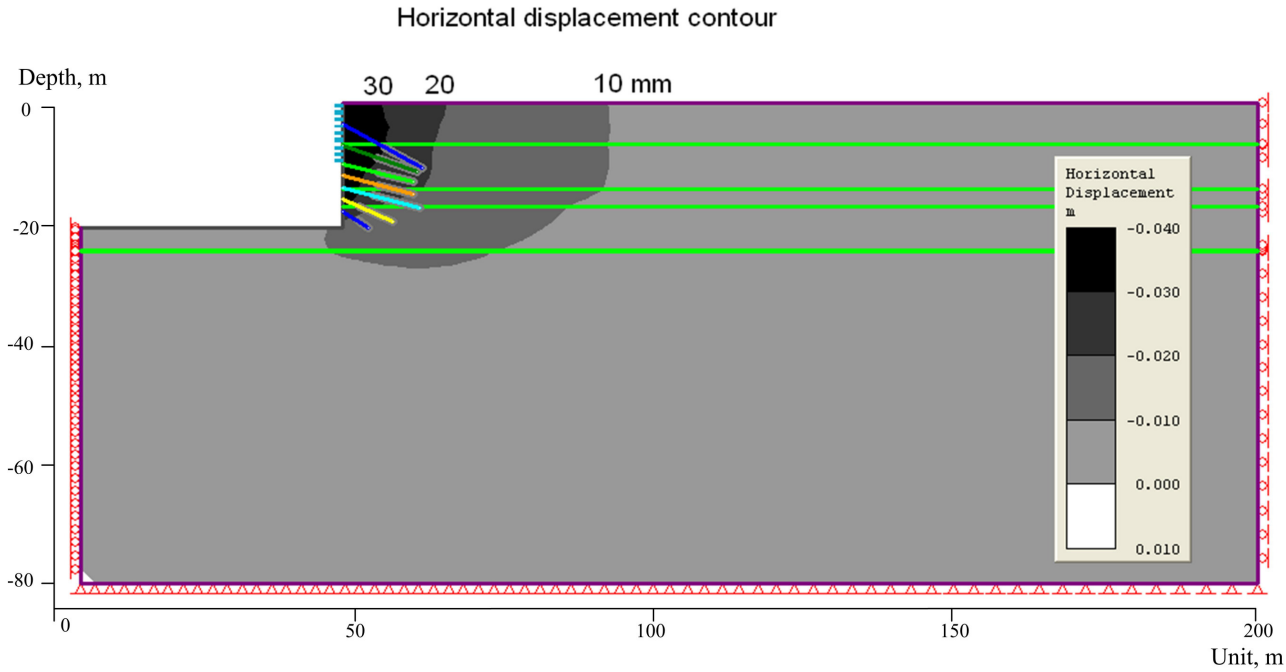

Figure 12b. Horizontal displacement contour (calculated) at #5 and #6

3.1.2 Overall Deformation and Yielding Zones

Figures 8, 9 and 10 provide further detailed deformation results from the numerical analysis. In Figure 8, the displacement contour shows a clear discontinuity at the shear band, suggesting considerable interface slip. This interface slip contributed to substantial displacement away from the excavation face. The calculated lateral

movement is 40 mm at a distance of about 10 m, 20 mm at a distance of 40 m approximately two times of the depth of excavation. Figure 9 shows the plastic zone calculated from the finite element model. It can be clearly seen that the whole shear band layer is in a shear yielding state, consistent with the large lateral movement in this layer. Some tension yielded elements occur close to the bonded portion of anchors. However, no continuous yielding zone has been developed along any anchors, suggesting that all anchors work normally.

Figure 10 shows the distribution of displacement vectors in the soil and the rock mass. It can be seen that the horizontal movement dominates the displacement behind the excavation face. In the vertical direction, a maximum settlement of 13.3 mm occurs at a distance of about 10 m from the excavation face. The calculated maximum base heave is 28 mm, at a distance of about 12 m from the excavation face.

3.1.3 Lateral Stress Release

During excavation, lateral *in-situ* stress is released. Figure 11 shows the distribution of σ_h in the weak zone/layer at a depth of 16m after the excavation.

3.2 Numerical Model Accounting **Only** for Weak Zone (Neglecting Shear Band)

Figure 12a shows the measured deflections at the inclinometers #5 and #6. No significant slip or discontinuous lateral movement can be seen, suggesting that the influence of shear band at these locations is insignificant. Accordingly, a modified numerical model was constructed using exactly same parameters as shown above except that the shear band material properties were replaced with the lower rock layer properties.

The calculated and measured deflections at the inclinometers #5 and #6 are compared in Figure 12a. The agreement appears reasonable in term of both magnitude and distribution. It may be noted that the calculated deflection at the inclinometer bottom (at a depth of 30 m) is about 10 mm, suggesting that the actual lateral movement may be about 10 mm larger than those measured by inclinometer.

Figures 12b presents the calculated displacement contour at #5 and #6. The calculated lateral movement is 30 mm at a distance of about 7 m, 20 mm at a distance of about 17 m, 10 mm at a distance of 40 m approximately two times of the depth of excavation. Comparison between Figure 12b and Figure 8 may highlight that the presence of the shear band introduces: 1) a significant interface slip and consequently a discontinuity displacement contour, and 2) relatively larger magnitude of lateral displacement and 3) far-reach influenced zone behind of the excavation face.

4 SUMMARY AND CONCLUSIONS

Analyses of the displacements resulting from the excavation at The Bow have been carried out for the North Wall (IO 3 and IO 4) and East Wall (IO 5 and IO 6). A study of the excavation sequence showed that at these locations, simulation of excavation performance may be carried out in 2-D plane strain analyses. The rock parameters used were from results of laboratory tests on samples recovered at the bottom of the excavation and interpreted for other zones using data from point load tests. The largest uncertainty, however, is the initial state of horizontal stresses in the rock mass and assumption had to be made based on experience elsewhere. In spite of the limitations, however, the following tentative conclusions may be made:

(1) The results of the analyses produced maximum displacement in magnitude and location consistent with results of inclinometer monitoring.

(2) The presence of the weak layer contributed significantly to the total maximum displacements and its effect on excavation performance should be taken into account in future design where appropriate.

(3) The large displacements occurring in the shear band as slippage resulted in far field deformation at substantial distance from the anchor wall.

(4) The calculated maximum heave at the bottom of the excavation is approximately 28 mm and maximum settlement behind the wall approximately 13 mm.

To advance the state of knowledge in deep excavation in the Calgary area, measurement of the state of stresses in the rock formation must be carried out.

REFERENCES

AMEC 2006. *Supplementary Geotechnical Investigation Proposed EnCentre Tower 5 Avenue SE and Centre Street*, Calgary, Alberta, AMEC Earth & Environmental, Calgary, Alberta.

Kwan Yee Lo, Silvana Micic, Thomas Larder, and Matthew Janes, (2009) "Geotechnical properties of a weak mudstone in downtown Calgary. *Proc. 62nd Canadian Geotechnical conference*, GeoHalifax

R.W.I. Brachman, I.D Moore, K.Y. Lo, (1998) "Analysis and performance of a shoring system with tie-back anchors" *Proc. 51st Canadian Geotechnical conference*, Edmonton, Albeta, Oct. 4-7, Vol1 pp 439-446.

Rocscience, 2008 *PHASE2 v.6.027 user's guide*. Rocscience Inc. Toronto, Ont.